

Supporting Information

MOLECULAR AND DIMENSIONAL PROFILING OF HIGHLY PURIFIED EXTRACELLULAR VESICLES BY FLUORESCENCE FLUCTUATION SPECTROSCOPY

**Romain Wyss,^{§,#} Luigino Grasso,^{§,#} Camille Wolf,[§] Wolfgang Grosse,[§] Davide Demurtas,[‡]
and Horst Vogel^{*,§}**

[§]Laboratory of Physical Chemistry of Polymers and Membranes, Ecole Polytechnique Fédérale de Lausanne, Station 6, 1015 Lausanne, Switzerland

[‡]Interdisciplinary Center for Electron Microscopy, Ecole Polytechnique Fédérale de Lausanne, Station 12, 1015 Lausanne, Switzerland

*E-mail: horst.vogel@epfl.ch

TABLE OF CONTENTS

Experimental Section

Materials.

Cell culture.

Isolation of EVs.

Labeling of EVs.

Cryo-EM.

Formation of artificial lipid vesicles.

Acquisition of fluorescence fluctuations.

Analysis of fluorescence fluctuations.

Figure S1: Size-exclusion chromatography.

Figure S2: Single fluctuation analysis of artificial lipid vesicles.

Figure S3: Fluorescence fluctuation spectroscopy of free anti-CD63-FITC antibodies.

Figure S4: Comparison of EV size distributions measured with SFA and cryo-EM.

References

Experimental Section

Materials: Dulbecco's phosphate-buffered saline (D-PBS, Life Technologies), DMEM/F-12+ GlutaMAX (Life Technologies), Newborn Calf Serum (NBCS, Life Technologies), Alexa Fluor 488 (Life Technologies), Anti-CD63-FITC (Sigma-Aldrich), 1-palmitoyl-2-oleoyl-*sn*-glycero-3-phosphocholine (POPC, Avanti Polar Lipids), 1-oleoyl-2-[12-[(7-nitro-2-1,3-benzoxadiazol-4-yl)amino]dodecanoyl]-*sn*-glycero-3-phosphocholine (NBD-PC, Avanti Polar Lipids).

Cell culture: HEK293T cells were grown in DMEM/F-12 + GlutaMAX medium supplemented with 10% NBCS (unless otherwise stated) in a humidified 5% CO₂ atmosphere at 37°C.

Isolation of EVs: EVs were isolated from the conditioned medium (CM) of $\sim 40 \times 10^6$ cultured cells maintained in serum-free medium during the last 48 h. The CM was first centrifuged at 300 *g* for 4 min followed by filtration through a 0.22 μ m pore-sized filter. EVs were pre-purified and concentrated by UF using a 100 kDa molecular weight cutoff (MWCO) Amicon Ultra-15 centrifugal filter unit (Millipore), resuspended in D-PBS and concentrated again by UF to a volume of approximately 250 μ l. EVs were further purified by SEC using a Superose 6 10/300 GL column (GE Healthcare) equilibrated in D-PBS with an ÄKTA-Purifier system (GE Healthcare). EV-containing fractions were identified by absorption at $\lambda = 280$ nm and concentrated to the desired volume with a 100 kDa MWCO Amicon Ultra-4 centrifugal filter unit (Millipore). Connection of a RF-20A Prominence spectrofluorimetric detector (Shimadzu) allowed monitoring of fluorescence during elution ($\lambda_{\text{ex}} = 485$ nm, $\lambda_{\text{em}} = 515$ nm).

Labeling of EVs: Immunolabeling of EVs was achieved by incubation of anti-CD63-FITC antibodies (1:50 dilution) for 1 h. Unbound antibodies were then removed by SEC as described in the previous section.

Cryo-EM: The samples were prepared in a controlled environment using a vitrification system Vitrobot (FEI, Mark IV). The chamber temperature was held at 22-23°C, and the relative humidity was kept close to saturation (100%) to prevent water evaporation from the sample. A 5 μ l sample drop was placed on a Lacey carbon film grid (Agar Scientific) and blotted with filter paper to obtain a thin liquid film. The grid was then rapidly plunged into liquid ethane at -180°C. The grids containing the vitrified specimens were stored in liquid nitrogen and transferred into a Tecnai F20 microscope using a Gatan 626 cryo-holder and its workstation. The acceleration voltage was 200 kV and the working temperature was kept below -170°C. The images were recorded digitally with a Eagle camera 4k x 4k (FEI) under low-dose conditions with an underfocus of approximately -2 μ m and 25'000x-50'000x of magnification.

Formation of artificial lipid vesicles: Unilamellar vesicles were prepared in three steps: (i) The lipid mixture POPC:NBD-PC in a weight ratio of 99.5:0.5 was dissolved in chloroform and a dry lipid film was generated by placing the recipient in a rotary evaporator (Rotavapor, Büchi) at 300 mbar overnight. (ii) Water was poured onto the dry lipid film to give a lipid concentration of 1-2 mg/ml and vortexed for 1 min. (iii) The formed large multilamellar vesicles were disrupted by mechanical extrusion. Using a Mini-Extruder (Avanti Polar Lipids), the lipid solution was forced to pass through polycarbonate filters (Whatman) with various pore sizes (30, 100 and 400 nm). To achieve a narrow size distribution, the solution was passed 40x through the filter. At the end of the downsizing process, the vesicle solutions were transparent.

Acquisition of fluorescence fluctuations: For each fluorescently labeled sample, a droplet of 40 μ l was deposited on a coverglass #1 (Menzel-Gläser) mounted on a LSM 510 Meta laser scanning microscope equipped with a ConfoCor 3 unit (Carl Zeiss MicroImaging GmbH). The 488 nm laser line of an Ar-ion

laser was used to excite the fluorescent probes and a 40x/1.2NA water-immersion objective focused the laser beam to a diffraction-limited spot and collected the emitted photons. The incident irradiance was adjusted with an acousto-optical tunable filter (AOTF). Fluorescence time traces were recorded for 30 x 10 s and stored with a minimal binning time of 100 μ s and used for generating autocorrelation curves with a built-in photon correlator.

Analysis of fluorescence fluctuations: The translocation of fluorescent species through the observation volume leads to fluorescence fluctuations, which can be analyzed both in time and amplitude. In a first step, the autocorrelation function (eq. 1) was used to analyze these fluctuations:

$$G(\tau) = \frac{\langle F(t) \cdot F(t+\tau) \rangle}{\langle F(t) \rangle^2} \quad (1)$$

the brackets denote a time average, $F(t)$ the fluorescence signal at time t and τ the lag time. The autocorrelation data were further fitted (eq. 2) with a 3-D diffusion model comprising one or two components:

$$G(\tau) = \frac{1}{N} \left[f \cdot \left(\frac{1}{1 + \frac{\tau}{\tau_{D1}}} \right) \cdot \left(\frac{1}{1 + \frac{\tau}{S^2 \cdot \tau_{D1}}} \right)^{\frac{1}{2}} + (1-f) \cdot \left(\frac{1}{1 + \frac{\tau}{\tau_{D2}}} \right) \cdot \left(\frac{1}{1 + \frac{\tau}{S^2 \cdot \tau_{D2}}} \right)^{\frac{1}{2}} \right] \cdot \left(1 + \frac{T}{1-T} e^{-\frac{\tau}{\tau_T}} \right) \quad (2)$$

N is the mean number of fluorescent particles present in the observation volume, τ_{D1} and τ_{D2} the translational diffusion times of species 1 and 2, respectively, S the structural parameter representing the ratio of long axis radius (w_z) and short axis radius (w_{xy}) of the observation volume, and f the fraction of species 1. An additional term representing the triplet state of the fluorescent probe, where T is the triplet fraction and τ_T the triplet time, was employed only if indicated. A detailed mathematical treatment of equation 1 can be found elsewhere^{1,2}. The value of the short axis radius was calibrated using the fluorescent probe Alexa Fluor 488 of known diffusion coefficient D , and the relation that links τ_D and D (eq. 3):

$$\tau_D = \frac{w_{xy}^2}{4D} \quad (3)$$

Finally, the hydrodynamic diameter D_H of each species was determined by the Stokes-Einstein relation (eq. 4):

$$D = \frac{2k_B T}{6\pi\eta D_H} \quad (4)$$

k_B is the Boltzmann constant, T the temperature in Kelvin and η the viscosity of the solution.

In a second step, the single fluorescence events present in the time recordings were selected and

analyzed by single fluctuation analysis (SFA) using a home-written IGOR Pro (WaveMetrics) automatic evaluation routine. The program analyzes the fluorescence signal storing its mean value and its standard deviation. Alternatively, the mean and the standard deviation can be manually investigated and stored. Candidates for translocation events are identified when the signal rises above a user-defined multiple of standard deviation above the baseline signal. The start and end points of an event are further refined by looking backward/forward at data points which fall in 1.5x the standard deviation of the baseline signal. The user has the possibility to discard identified events whose time duration is shorter than a user-defined threshold time. At the end of the routine, each vesicle translocation event is described by its duration and its fluorescence intensity as well as the frequency. Results are presented in 2-dimensional probability distribution functions (2D-PDFs) of fluorescence intensity versus translocation time and in individual histograms of these two parameters. Finally, the translocation times were expressed in size with the help of equation 3 and 4.

Figure S1

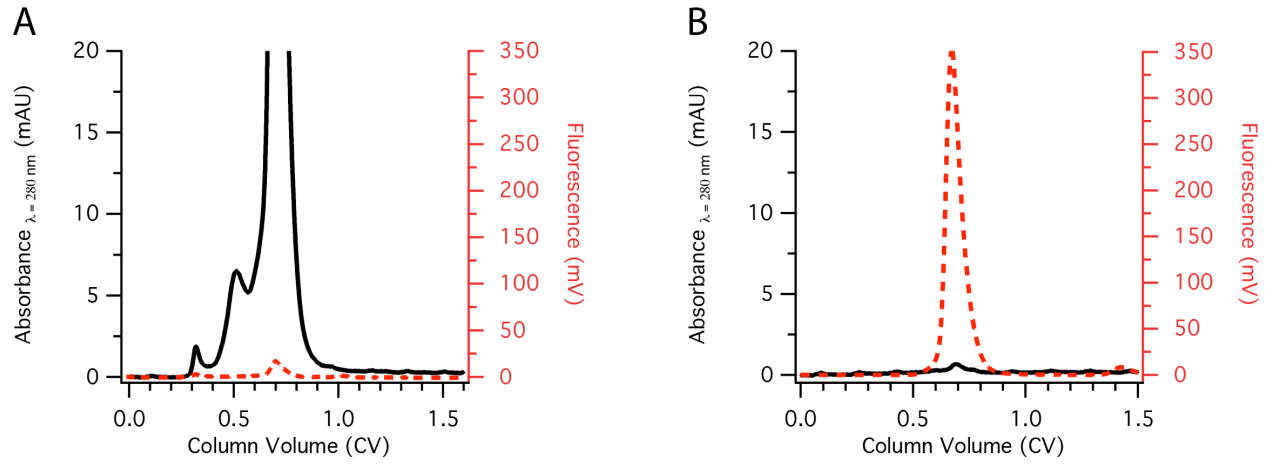


Figure S1: Size-exclusion chromatography. (A): Typical SEC elution profiles of unlabeled EVs released from HEK293T cells. The absorbance at 280 nm (black) corresponds to the total amount of protein. The fluorescence signal detected in the fluorescence chromatogram (excitation at 485 nm, emission at 515 nm; dashed red) was due to autofluorescence, negligible in our experimental conditions. (B): Typical SEC elution profile of pure Anti-CD63-FITC; the absorbance is given in black and the corresponding specific fluorescence of the antibody in dashed red.

Figure S2

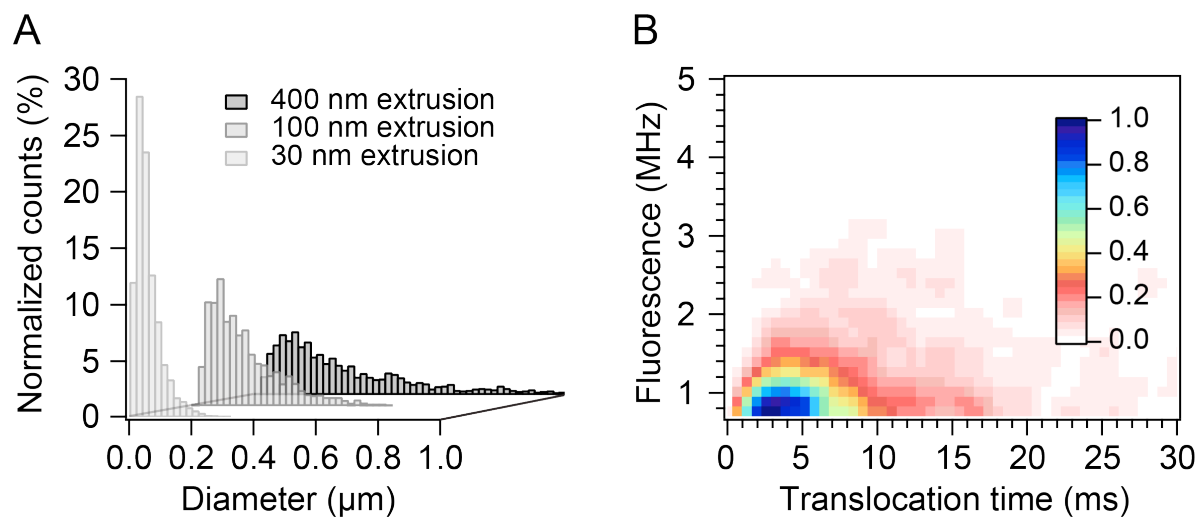


Figure S2: Single fluctuation analysis of artificial lipid vesicles. (A): Waterfall plot of histograms of the hydrodynamic diameters of 3 vesicle preparations extruded through 30, 100 and 400 nm pore filters, respectively. (B): 2D-PDF of fluorescence intensity versus translocation time for the 400 nm vesicle preparation.

Figure S3

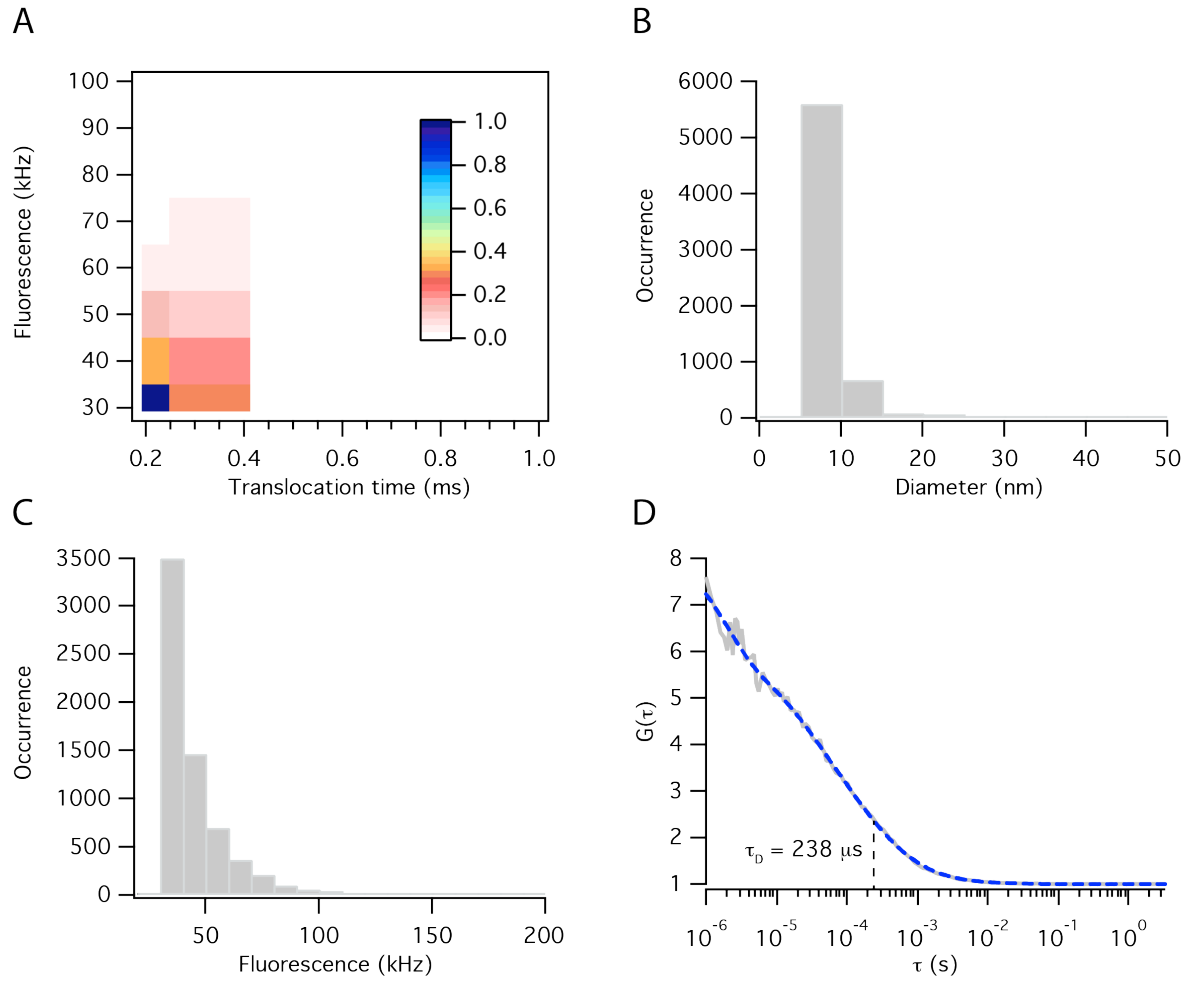


Figure S3: Fluorescence fluctuation spectroscopy of free anti-CD63-FITC antibodies. (A): 2D-PDF of fluorescence intensity versus translocation time for anti-CD63-FITC antibodies. (B): Histogram of the calculated hydrodynamic diameter. (C): Histogram of the measured fluorescence intensity. (D): ACF (grey solid line) was fitted with a 3-dimensional 2-components diffusion model taking into account the triplet state (blue dashed line).

Figure S4

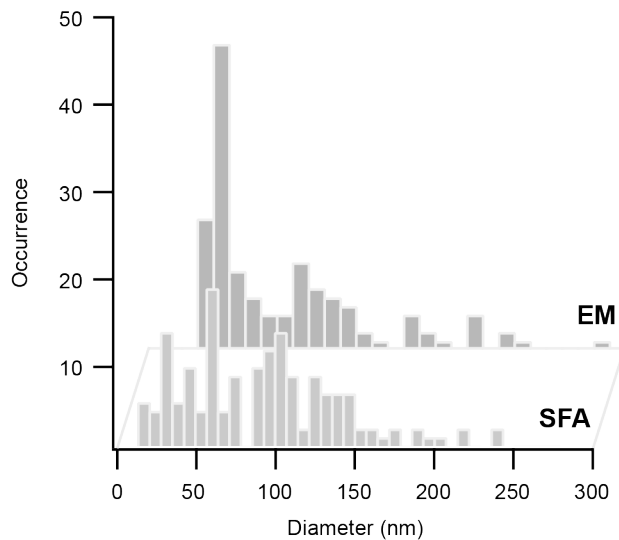


Figure S4: Comparison of EV size distributions measured with SFA and cryo-EM. *Waterfall plot of histograms of the hydrodynamic diameters of EVs released from HEK293T cells determined by SFA and cryo-EM.*

References

- (1) Elson, E. L. *Biophys J* **2011**, *101*, 2855–2870.
- (2) Maiti, S.; Haupts, U.; Webb, W. W. *Proc. Natl. Acad. Sci. U. S. A.* **1997**, *94*, 11753–11757.